**Advanced Steel Construction** – Vol. 21 No. 6 (2025) 476–487
**DOI:**10.18057/IJASC.2025.21.6.1


# EVALUATION METHOD FOR MECHANICAL PROPERTIES OF CORRODED ANGLE STEEL IN TRANSMISSION TOWERS

Wen-Qiang Jiang [1, 2, 3, *], Heng Zhang [1], Tong-Tong Dai [1, 2, 3], Yu-Cheng Guo [1] and Yue-Ming Zhong [1]

[1] *Department of Mechanical Engineering, North China Electric Power University, Baoding, China*
[2] *Hebei Engineering Research Center for Advanced Manufacturing & Intelligent Operation and Maintenance of Electric Power Machinery，North China Electric Power University, Baoding, China*
[3] *Hebei Key Laboratory of Electric Machinery Health Maintenance & Failure Prevention, North China Electric Power University, Baoding 071003, China*
** (Corresponding author: E-mail: wenqiang.jiang@ncepu.edu.cn)*

**ABSTRACT**

Corrosion inevitably exists in transmission towers that have been in long-term field service. In order to study the corrosion properties of tower angle steel, the corroded steel specimens were prepared by accelerated corrosion test in this research. Combined with surface roughness and tensile test of the corroded specimens, the corrosion process of the steel specimens was explored, the degradation law of mechanical properties of the corrosion specimens was analyzed. Then, a method for estimating the corrosion rate of steel members by residual thickness was proposed. Moreover, the relationship between mechanical properties of corroded steel members and corrosion rate and surface roughness was established. The results show that the corrosion rate, the maximum pit depth and the maximum pit depth to width ratio are highly correlated with the strength degradation of corroded specimens. It is most effective to evaluate the strength of the specimens by the maximum pit depth.

**ARTICLE HISTORY**

Received: 5 July 2024
Revised: 27 February 2025
Accepted: 2 March 2025

**KEYWORDS**

Angle steel member;
Corrosion;
Surface roughness;
Tensile test;
Evaluation methods



## 1. Introduction

As the main material of transmission tower, structural steel is susceptible to corrosion during long-term service due to environmental and climatic factors [1,2]. Corrosion reduces the load-bearing capacity of components and affects the overall structural safety of transmission towers. Therefore, it is necessary to carry out regular inspections and evaluate the residual load-carrying capacity of corroded components to determine subsequent maintenance methods [3,4].

In the natural environment, the corrosion process of structural steel is relatively slow. It takes a long time to produce obvious corrosion phenomena [5]. Therefore, the accelerated corrosion method has been widely used to prepare corrosion specimens [6-7]. For the corrosion simulation of atmospheric environment, the commonly used methods for accelerating corrosion mainly include electrochemical accelerated corrosion method and salt spray test method. Many scholars have proved that these two methods are feasible. For example, Bazan A et al. [8] immersed steel bars with peripheral auxiliary electrodes in NaCl solution to study the effect of centripetal stress on structural properties during the corrosion of steel bars. Si Qi et al. [9] placed steel structure specimens in electrolytic corrosion solution to simulate atmospheric corrosion and analyzed the surface characteristics of corroded steel plates based on surface roughness theory and fractal theory. Cheng Ding et al. [10] conducted a neutral salt spray corrosion test on mild steel specimens and discussed the kinetic law of corrosion of mild steel. Deliang Kong et al. [11] conducted a neutral salt spray accelerated corrosion test on steel plates. An autocorrelation function model of the corrosion depth random field model is proposed based on the surface profile and 3D data of corroded steel plate. Guangchong Qin et al. [12] adopted NaCl solution spray to simulate coastal corrosion environment, the natural corrosion was well simulated within the acceptable error range. Compared with the electrochemical accelerated corrosion method, salt spray test can better simulate the natural environment, the experimental operation is simple and the results have high reliability and repeatability. Therefore, the salt spray test method will be used to prepare corrosion specimens in this research.

Corrosion rate is an important parameter to characterize the degree of corrosion damage of structural steel, which is calculated from the mass loss rate before and after corrosion of components [13-14]. The effect of corrosion rate on mechanical properties of corroded steel plate has been studied deeply by many scholars. Yuchen Ou et al. [15] conducted tensile tests on natural and artificial corroded steel bars respectively and obtained the relationship between tensile properties and corrosion rate. Zhenye Chen et al. [16] obtained high-performance steels with different degrees of corrosion through accelerated corrosion experiments with salt spray. The relationship between mechanical properties and corrosion rate was discussed by tensile test. Feng Liang et al. [17] investigated the relationship between mechanical properties and corrosion rate of S420 steel hull plates through accelerated corrosion cycle experiment and ultimate strength experiment. However, it is challenging to dismantle and weigh transmission tower components, making it difficult to obtain the corrosion rates. To solve this problem, a new method for evaluating the corrosion rate of corroded components by maximum residual thickness is proposed in this paper.

Moreover, the research shows that the surface morphology has a great influence on the residual mechanical properties of corroded components [18], especially in the aspects of deformation capacity [19-22] and fatigue behavior [23-26]. Naftary G et al. [27] obtained corroded steel specimens with different corrosion degrees through underwater accelerated corrosion tests and established a regression model for ductility estimation based on surface roughness in order to estimate the residual ductility of steel plates by roughness characteristics. Wei Wang et al. [28] established a mathematical model of the surface contour height of corroded steel based on the spectrum representation method and proved the reliability of the mathematical model taking standard deviation, arithmetic mean height and maximum height as evaluation indexes. Haipeng Song et al. [29] investigated the fatigue failure behavior of pre-corroded aluminum alloy based on experimental information such as three-dimensional rust morphology and established a data-driven fatigue life prediction model based on machine learning. Songbo Ren et al. [30] used statistical analysis to study the surface topography parameters of corroded steel and proposed a fractal reconstruction model of corroded steel surface based on W-M function. Therefore, it is necessary to consider the surface morphology parameters such as roughness when evaluating the residual mechanical properties of corroded tower members. However, the existing research results on surface morphology are mainly aimed at specific components under specific corrosion environment and lack of universality. The material and environment of transmission tower angle steel are special and their corrosion condition may be different from that of ordinary steel. Therefore, the surface morphology of transmission tower angle steel members during corrosion is deeply studied in this paper.

This paper aims to explore the corrosion process of angle steel with accelerated corrosion experiments and analyze the changes of mechanical index, corrosion rate and surface characteristic parameters during corrosion. In view of the difficulty of angle steel disassembly, evaluation methods of corrosion degree and mechanical properties are proposed, which provides a theoretical basis for practical engineering application. The layout of the paper is as follows. In section 2, the accelerated corrosion experiment is introduced, including the acquisition of experimental materials, experimental equipment and experimental methods. The experimental results are analyzed and a method for evaluating the corrosion rate of corroded steel by residual thickness is proposed in section 3. In section 4. Mechanical properties of corroded steel are evaluated by different evaluation indexes and the reliability is compared. Finally, Section 5 and Section 6 provide the discussion and conclusion respectively.

## 2. Experimental scheme

The section mainly introduces the experimental process. Firstly, standard tensile specimens were prepared by cutting angle steel, NaCl solution was used to simulate the atmospheric corrosion environment with high salinity, specimens with different corrosion rates were obtained by controlling the corrosion duration. Then the profile curve data of the corroded specimen surface were measured with a profile measuring instrument. Finally, the tensile test of the specimen was carried out.

### *2.1. Accelerated corrosion test*

The purpose of this study is to explore the degradation of transmission tower components due to corrosion during service. Given that angle steel is a common component of the tower, the steel plate was obtained by cutting angle steel in the way shown in Fig.1. In order to facilitate the subsequent tensile test, the steel plate was cut and processed into the standard tensile specimen as shown in Fig.2. The material used in the test is hot-rolled Q235 steel. Q235 steel is a carbon structural steel, its chemical composition is: carbon content between 0.14% and 0.22%, silicon content is less than 0.30%, manganese content is between 0.30% and 0.70%, sulfur content is less than 0.050%, phosphorus content is less than 0.045%.

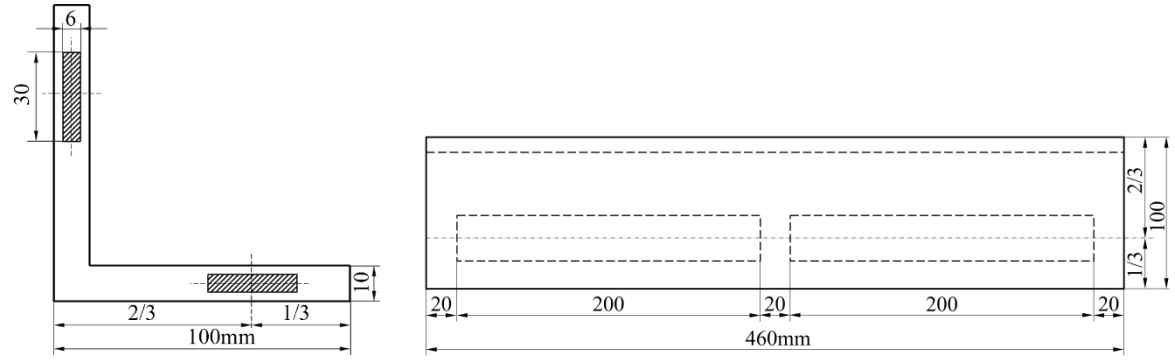


(a) Angle steel front view (b) Angle steel top view

**Fig. 1** Specimen sampling

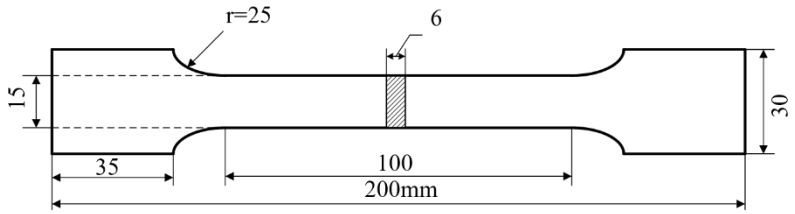


**Fig. 2** Specimen size

In order to prepare corroded specimens, saturated sodium chloride solution was sprayed to simulate the environmental conditions of the coastal transmission tower, so as to accelerate the corrosion rate of the specimen and shorten the corrosion period. The experiment steps are as follows: (1) The accelerated corrosion experimental device is shown in Fig.3. A salt spray chamber with built-in specimen frames was constructed using plastic film and support. At the same time, 8 timed quantitative salt spray nozzles were arranged on both sides of the placing frame. (2) The spray settings of the salt spray nozzle are shown in Table 1. In order to ensure uniform corrosion on the surface of the specimen, the solution should be penetrated to the surface each time. (3) At the same time, the specimens were periodically turned over every 5 days to ensure consistent corrosion on both sides of the specimens.

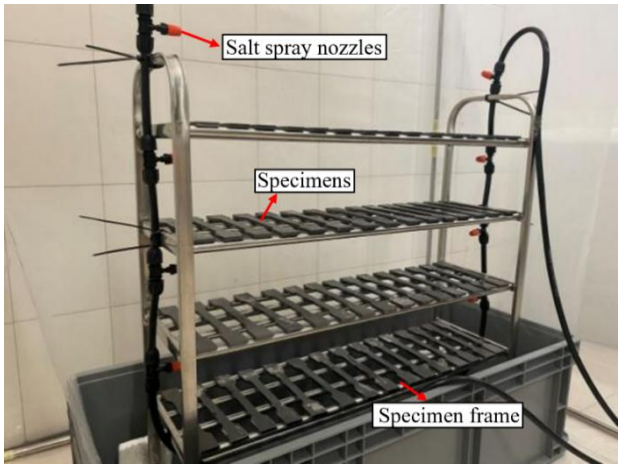


**Fig. 3** Accelerated corrosion experimental device

**Table 1**
Salt spray rules

| Interval time/hour | Spray time/min | Spray volume/liter |
|---|---|---|
| 6 | 1 | 5.5 |

The processing steps of the specimens during the experiment are as follows: (1) Before the experiment, a total of 60 specimens were randomly divided into 4 groups on average, the predetermined corrosion duration of each group was shown in Table 2. After weight and size were measured, each group of specimens was placed on the corresponding specimen rack in batches. (2) For specimens that reached the predetermined corrosion days, they were removed and soaked in a hydrochloric acid solution to dissolve and wash away loose rust on the surface of the rusty parts. In order to prevent pickling damage to the corroded surface of the specimen, 10% dilute hydrochloric acid was used for pickling, the specimens were taken out every 10 minutes, the surface was wiped with a soft cloth. Repeat the above steps until the corrosion products on the specimen surface were completely removed. (3) After pickling, the specimens were placed in calcium hydroxide solution to neutralize the residual pickling solution. (4) After the specimens were cleaned and dried, the size and weight of each corroded specimen were measured. The corrosion specimen before and after rust removal is shown in Fig.4.

**Table 2**
Predetermined corrosion time of specimens

| Group | Corrosion days/d |
|---|---|
| A | 30 |
| B | 50 |
| C | 70 |
| D | 90 |


**Fig. 4** Comparison of test pieces before and after rust removal

### 2.2. Surface topography measurement

The steps for extracting the surface topography data of corroded steel are as follows: (1) After the accelerated corrosion experiment, 3 specimens were randomly selected from each group A, B, C and D and numbered as shown in Table 3. (2) Three lines were selected equidistant from each of the two surfaces of the specimen, six lines were selected in total as shown in Fig.5. (3) Sanfeng FTA-H4C3000-D profile measuring instrument as shown in Fig.6 was used to measure and record the surface topography data along the selected lines. The sampling length of the instrument is 80mm, the sampling interval is 10μm and the sampling number is 8000. The two-dimensional contour curve of the measured specimen is shown in Fig.7.

**Table 3**
Contour measurement test piece group

| Group | No. |
|---|---|
| A | A1 A2 A3 |
| B | B1 B2 B3 |
| C | C1 C2 C3 |
| D | D1 D2 D3 |

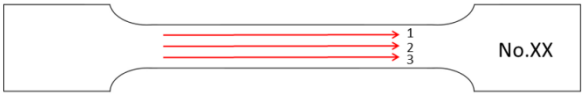


**Fig. 5** Scanning position of specimen surface

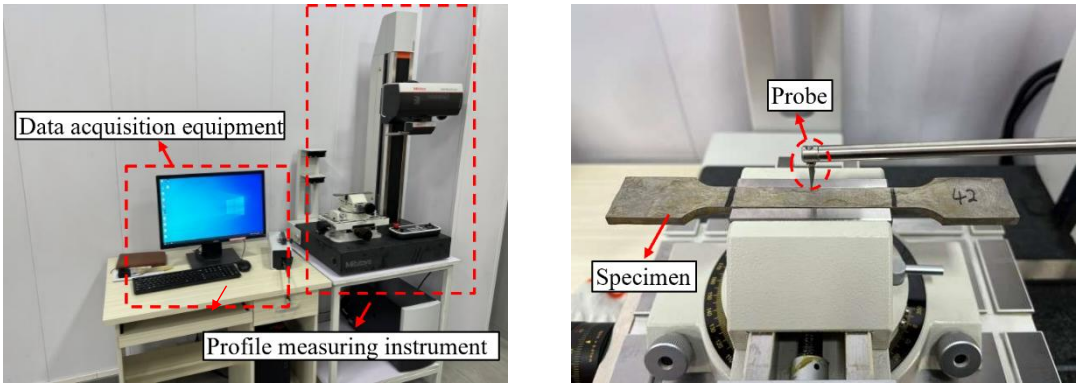


**Fig. 6** Sanfeng FTA-H4C3000-D probe profilometer

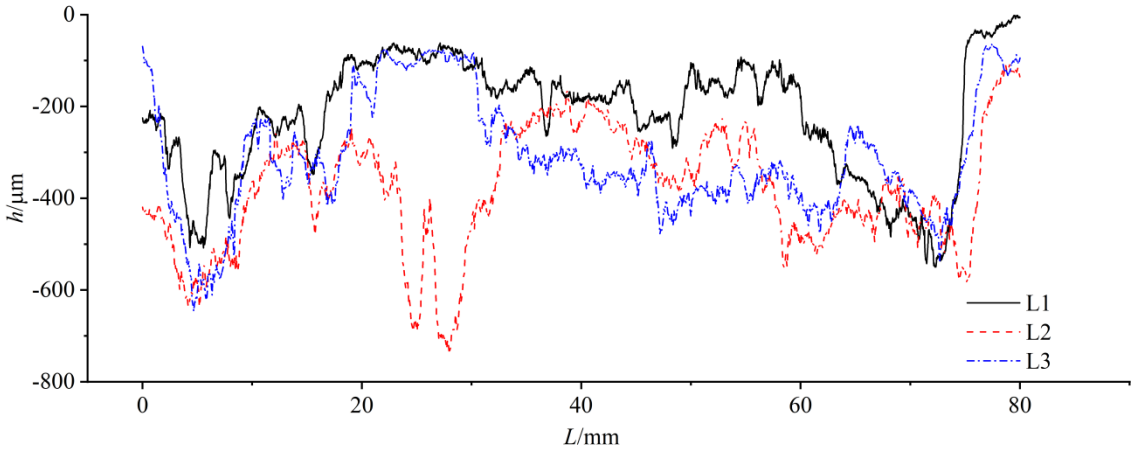


**Fig. 7** Surface profile curve of specimen D1

### 2.3. Room temperature tensile test

MTS E45 electronic universal testing machine as shown in Fig.8 was used for the tensile test at room temperature. The experimental steps are as follows: (1) Three uncorroded specimens (numbered 01, 02 and 03 respectively) and 12 corroded specimens with contour scanning above, a total of 15 specimens, were selected for the tensile test. Before the experiment, the marking distance with an initial length of 50mm was set on the specimen (2) During the test, the system automatically collected and recorded the force and deformation in real time through the testing machine and the extensometer beam. The loading rate of the tensile test was set to 5mm/min until the specimen was pulled apart. (3) At the end of test, remove the extensometer. The stress-strain curves were obtained by data acquisition equipment.

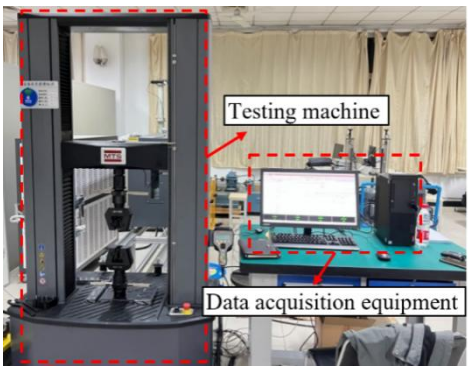


**Fig. 8** MTS E45 electronic universal testing machine

## 3. Experimental results and analysis

The section mainly introduces and analyzes the experimental results. Firstly, the change rule of corrosion rate with time was analyzed through accelerated corrosion experiment. Then, the surface morphology index of the specimen was extracted, the microscopic change process of surface was analyzed and the relationship between the thickness of each corrosion layer and the corrosion rate was established. Finally, according to the results of tensile test at room temperature, the variation of tensile properties with corrosion degree was analyzed.

### *3.1. The results of the accelerated corrosion test*

The weight of the specimen before and after the corrosion is $m_0$ and $m$ respectively, the equation of the corrosion rate $\eta$ is as follows:

$$\eta = \frac{m_0 - m}{m_0} \times 100\% \tag{1}$$

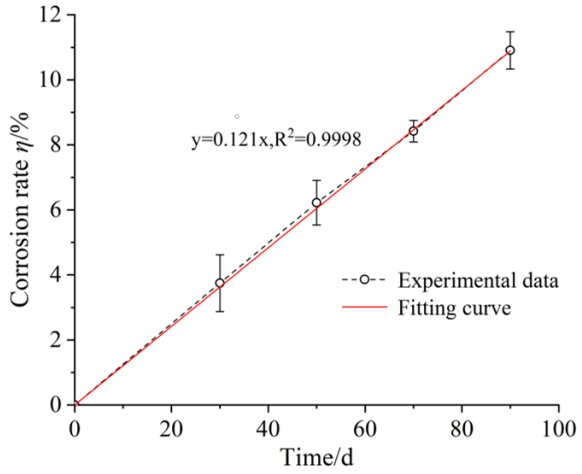


**Fig. 9** Relationship between corrosion rate $\eta$ and time

The corrosion rate of each specimen was calculated according to Eq. (1). The average corrosion rate of each group of specimens was taken as the corresponding corrosion rate under the corrosion duration of the group, the variation of corrosion rate over time was obtained, as shown in Fig.9. It can be seen the corrosion rate of the specimens changes roughly linearly with time when the corrosion rate is below 12%, that is, the specimens rust and lose weight at a constant rate.

### *3.2. The results of contour scan*

The surface roughness parameters of corroded specimens were calculated based on the two-dimensional profile curve scanned by the profile measuring instrument. In this paper, the main parameters of specimen surface roughness analysis are maximum section height ($R_t$), arithmetic average height ($R_a$) and root mean square height ($R_q$). $R_t$, $R_a$ and $R_q$ respectively represent the sum of the maximum peak height and maximum valley depth on the contour curve, the mean value of the absolute value of the contour offset on the datum length and the root-mean-square value of the contour offset on the reference length. The calculation equation of each roughness parameter is as follows:

$$R_t = \max(R_{pi}) + \max(R_{vi}) \tag{2}$$

$$R_a = \frac{1}{l}\int_0^l |Z(x)|dx \tag{3}$$

$$R_q = \sqrt{\frac{1}{l}\int_0^l Z^2(x)dx} \tag{4}$$

The surface roughness parameters of the specimen are calculated based on the profile curves shown in Fig.7 and the above equations. The position of the component before corrosion (corresponding to $h$=0 in Fig.7) is taken as the reference position and the coordinates of each measurement point are the offset at this point. The calculated surface roughness parameters of each component are shown in Table 4.

**Table 4**
Summary of corrosion rate and average roughness parameters of corroded parts

| No. | *t*/*d* | $\eta$/% | | Average roughness parameters | | | | | |
|---|---|---|---|---|---|---|---|---|---|
| | | | | $R_t$ | | $R_a$ | | $R_q$ | |
| A1 | | 4.30 | | 141.7 | | 337.0 | | 156.7 | |
| A2 | 30 | 4.46 | 4.31 | 209.1 | 159.9 | 386.9 | 348.0 | 216.1 | 170.5 |
| A3 | | 4.18 | | 129.1 | | 320.1 | | 138.6 | |
| B1 | | 5.44 | | 244.3 | | 521.9 | | 263.0 | |
| B2 | 50 | 5.40 | 5.59 | 281.0 | 265.6 | 598.8 | 575.7 | 302.3 | 284.4 |
| B3 | | 5.91 | | 271.4 | | 606.5 | | 288.0 | |
| C1 | | 8.56 | | 275.8 | | 601.4 | | 294.2 | |
| C2 | 70 | 8.26 | 8.56 | 282.9 | 276.2 | 600.1 | 633.6 | 299.3 | 299.0 |
| C3 | | 8.86 | | 270.0 | | 699.1 | | 303.4 | |
| D1 | | 11.04 | | 296.6 | | 732.7 | | 329.0 | |
| D2 | 90 | 11.36 | 11.02 | 304.3 | 290.0 | 723.7 | 702.0 | 332.8 | 318.8 |
| D3 | | 10.67 | | 269.1 | | 649.7 | | 294.5 | |

The relationship between surface roughness parameters and corrosion rate of corroded steel specimens is shown in Fig.10. It can be seen $R_a$, $R_q$ and $R_t$ increase with the increase of the corrosion rate when the corrosion rate of the specimen is between 0 and 6%. The growth rate of $R_a$, $R_q$ and $R_t$ slows down when the corrosion rate is between 6% and 11%, the growth of $R_a$ and $R_q$ almost stops and tends to be flat.

It can be seen that with the initial stage of steel surface corrosion process, dissolved oxygen reacts with steel surface materials, resulting in numerous rust pits. The steel surface starts to become rough and uneven, the surface roughness parameters increase. The corrosion becomes more and more serious with the deepening of the rust pit and the surface roughness parameters become larger. The corroded layer begins to seriously hinder the further contact between the corrosive medium and the material matrix when the corrosion process reaches a certain stage, preventing dissolved oxygen from reaching the uncorroded area of the steel, making it difficult for the steel to undergo oxidation reactions. As a result, the increase rate of the surface roughness parameters slows down.

In order to further study the deterioration of the mechanical properties of the specimens due to stress concentration caused by local rust pits on the surface of the corroded specimens, the size of the deepest rust pits on the corroded specimen was measured based on the results of surface profile scanning. The difference between the maximum depth value and the edge depth of the rust pit is denoted as the rust pit depth *d*. The edge distance between the two sides of the rust pit is denoted as the rust pit width *w*. The depth to width ratio of the rust pit is obtained by calculating *d*/*w*. The deepest rust pit was selected from the

contour curve for measurement as shown in Fig.11, the measurement data was recorded as shown in Table 5.

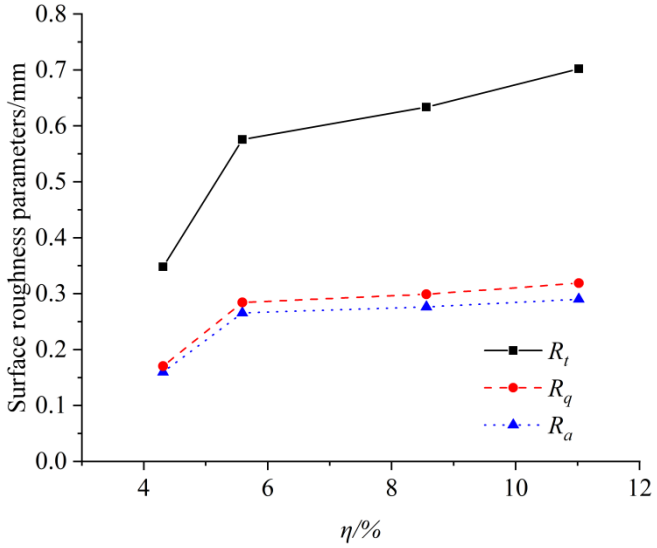


**Fig. 10** Relationship between $R_a$, $R_q$, $R_t$ and $\eta$

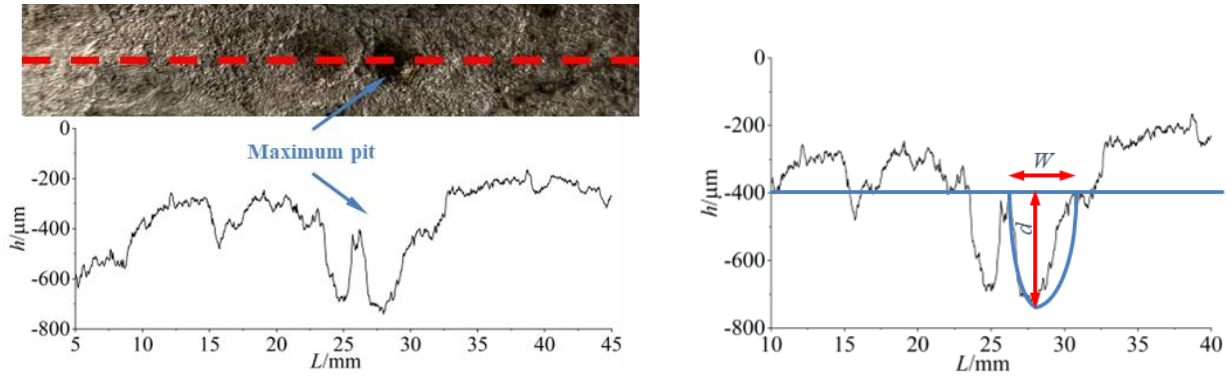


(a) Corrosion surface topography

(b) maximum rust pit size

**Fig. 11** Maximum rust pit measurement process

**Table 5**
Maximum rust pit size for each corrosion specimen (mean value of both sides)

| No. | *d*/μm | | *w*/μm | | *d*/*w* | |
|---|---|---|---|---|---|---|
| A1 | 132 | | 3668 | | 0.0361 | |
| A2 | 92 | 130 | 4825 | 4803 | 0.0193 | 0.0279 |
| A3 | 167 | | 5917 | | 0.0283 | |
| B1 | 202 | | 6080 | | 0.0357 | |
| B2 | 418 | 286 | 5284 | 5651 | 0.0419 | 0.0410 |
| B3 | 239 | | 5589 | | 0.0453 | |
| C1 | 278 | | 4909 | | 0.0607 | |
| C2 | 296 | 323 | 6822 | 7498 | 0.0485 | 0.0503 |
| C3 | 396 | | 10762 | | 0.0416 | |
| D1 | 420 | | 8660 | | 0.0515 | |
| D2 | 261 | 343 | 6856 | 8165 | 0.0402 | 0.0449 |
| D3 | 350 | | 8977 | | 0.0429 | |

According to Table 5, the relationship between the corrosion rate of the specimen and the maximum rust pit depth and the ratio of depth to width was obtained, as shown in Fig.12. It can be seen from the figure that the maximum rust pit depth and the depth to width ratio of the specimen increase significantly with the increase of the corrosion rate when the corrosion rate of the specimen is between 0% and 8%, which indicates that corrosion pits appear on the specimen surface at the initial stage of corrosion and deepen continuously. At a certain degree of corrosion, the rate of rust pits deepening slows down. Combined with Fig.10 and Fig.12, the corrosion rate at this stage is about 6%~8%. Meanwhile, it can be seen from Fig.12 (b) that the depth to width ratio of the maximum rust pit decreases when the corrosion rate is greater than 8%, which indicates that at this stage, the development of rust pits changes from longitudinal to transverse and the bottom of rust pits becomes wider. Rust pits gradually develop from the deeper pitting pits to the wide and deep ulcer pits. The analysis of the maximum rust pit not only verifies the corrosion process of steel obtained from roughness parameters in the previous paper, but also further reveals the development law of the microscopic characteristics of the corroded surface during the corrosion process.

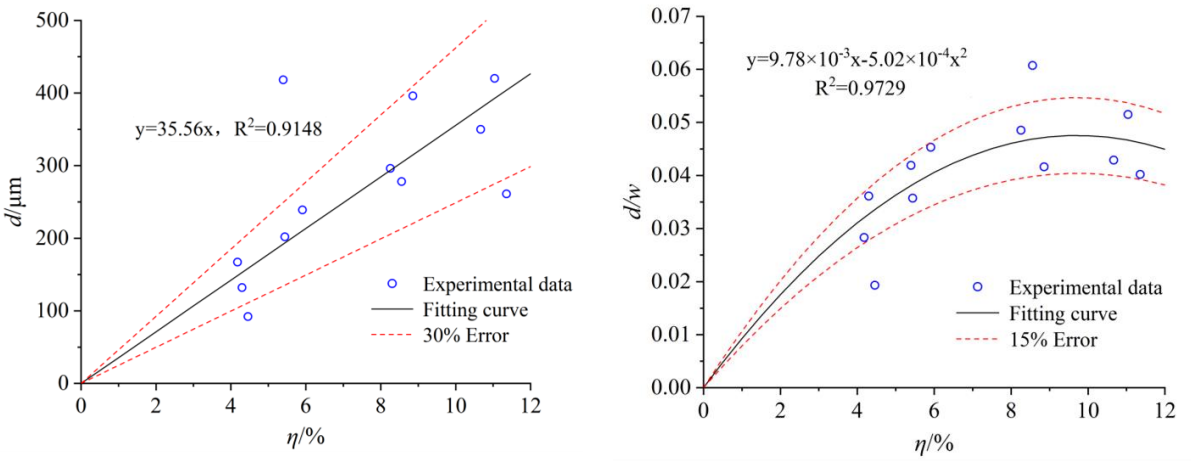


(a) Max rust pit depth (b) Max rust pit depth to width ratio

**Fig. 12** Relationship between corrosion rate and maximum rust pit size

### *3.3. Thickness of corrosion layer*

According to the morphology of the corroded steel surface, the cross-section of the corroded specimen is divided into regions as shown in Fig.13. It can be seen from the figure that the part where the steel is thinned as a whole due to rust is the uniform rust area. There is a non-uniform rust zone between the highest peak and the deepest valley of the steel surface profile. The uncorroded part in the middle of the material is the uncorroded area.

The original thickness $T_0$ of the specimen was measured before the test. The maximum residual thickness $T$ is the mean value of the measured thickness at five measuring points, as shown in Fig.14. The uniform rust layer thickness $h_1$ can be obtained by calculating the difference between the original thickness $T_0$ and the maximum residual thickness $T$. The thickness of the non-uniform corroded layer $h_2$ can be obtained from the height difference between the highest peak and the deepest valley of the profile curve of the corroded specimen. The total thickness of the rust layer $h_3$ is the sum of $h_1$ and $h_2$. The ratio of the thickness of each layer to the original thickness of the specimen is further calculated to obtain the proportion of each corroded layer. The thickness and proportion of each corrosion layer are summarized in Table 6.

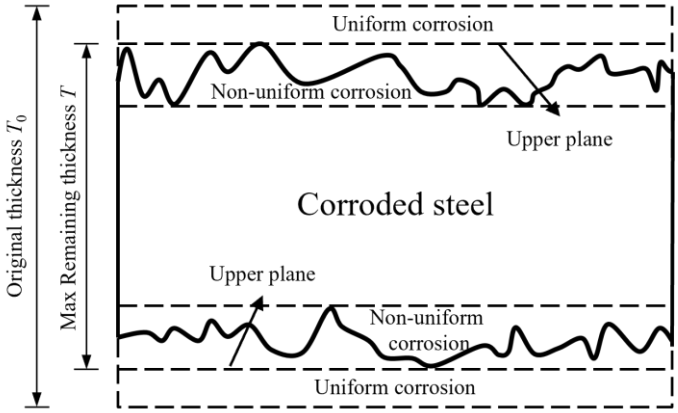


**Fig. 13** Division of each corrosion layer of corrosion test piece

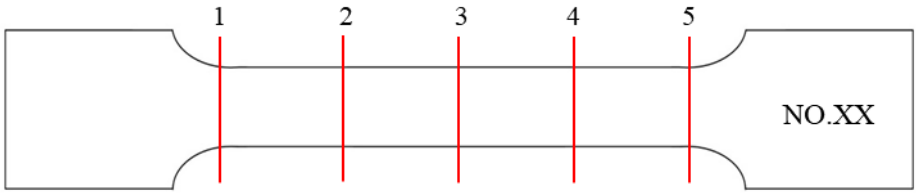


**Fig. 14** Measurement of maximum residual thickness

**Table 6**
Summary of thickness values of specimens and proportion of each layer

| No. | $T_0$ | $T$ | | $h_1$ | | $h_2$ | | $h_3$ | |
|---|---|---|---|---|---|---|---|---|---|
| A1 | 5.438 | 5.422 | 99.71% | 0.016 | 0.29% | 0.674 | 12.39% | 0.691 | 12.71% |
| A2 | 5.442 | 5.432 | 99.82% | 0.010 | 0.18% | 0.774 | 14.22% | 0.783 | 14.39% |
| A3 | 5.441 | 5.452 | 100.20% | -0.011 | -0.20% | 0.640 | 11.76% | 0.629 | 11.56% |
| B1 | 5.421 | 5.418 | 99.94% | 0.003 | 0.06% | 1.044 | 19.26% | 1.046 | 19.30% |
| B2 | 5.376 | 5.378 | 100.04% | -0.002 | -0.04% | 1.198 | 22.28% | 1.196 | 22.25% |
| B3 | 5.416 | 5.418 | 100.04% | -0.002 | -0.04% | 1.213 | 22.40% | 1.211 | 22.36% |
| C1 | 5.415 | 5.358 | 98.95% | 0.057 | 1.05% | 1.203 | 22.22% | 1.260 | 23.27% |
| C2 | 5.418 | 5.354 | 98.82% | 0.064 | 1.18% | 1.200 | 22.15% | 1.264 | 23.33% |
| C3 | 5.420 | 5.360 | 98.89% | 0.060 | 1.11% | 1.398 | 25.79% | 1.458 | 26.90% |
| D1 | 5.446 | 5.258 | 96.55% | 0.188 | 3.45% | 1.465 | 26.90% | 1.653 | 30.35% |
| D2 | 5.441 | 5.228 | 96.09% | 0.213 | 3.91% | 1.447 | 26.59% | 1.660 | 30.51% |
| D3 | 5.485 | 5.324 | 97.06% | 0.161 | 2.94% | 1.299 | 23.68% | 1.460 | 26.62% |

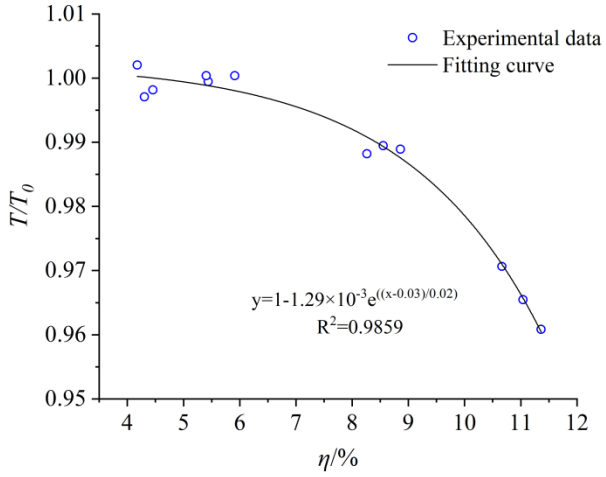


**Fig. 15** Relationship between $T/T_0$ and corrosion rate

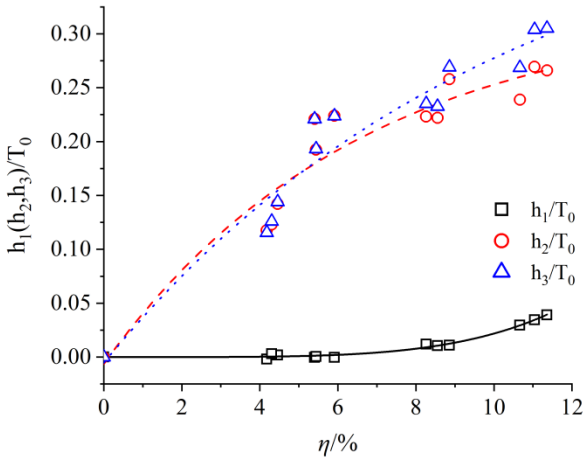


**Fig. 16** Relationship between $h_{1,2,3}/T_0$ and corrosion rate

According to the thickness data of each part of the specimen obtained in Table 6, the relationship between the ratio of maximum residual thickness $T/T_0$ and corrosion rate is shown in Fig.15. The fitting result obtained by the exponential growth function ExpGrow1 is shown in Eq. (5). The relationship between $h_{1,2,3}/T_0$ and rust rate is shown in Fig.16. It can be seen from the figure that the thickness of uniform rust layer increases slightly with the increase of rust rate, but the growth rate accelerates. The thickness of non-uniform rust layer increased greatly, but the growth rate slowed down. This indicates that the pit develops vertically in the early stage of corrosion. However, the depth of corrosion increases with the increase of the degree of corrosion, the gradually increasing corrosion products begin to hinder the contact between the corrosion medium and the steel matrix, making it difficult for the corrosion reaction to be carried out at deeper depths of the specimen. The development of rust pits changes from longitudinal to horizontal, which also confirms the development law of rust pits obtained from the change of surface roughness parameters. For the components in the steel structure that are not easy to disassemble, the maximum residual thickness can be measured, the corrosion rate can be calculated using the following equation. However, the corrosion rate cannot be calculated by the following equation for components with corrosion rate lower than 4% or higher than 12%.

$$\frac{T}{T_0} = 1 - 1.29\times10^{-3} e^{((\eta-0.03)/0.02)}, R^2 = 0.9859 \quad (5)$$

### *3.4. Results of tensile test*

The stress-strain curves of specimens obtained by tensile test are shown in Fig.17. It can be found from the figure that the mechanical properties of the same group of specimens have a certain discreteness. The dispersion of mechanical properties decreases and the degree of coincidence of stress-strain curves increases with the increase of corrosion rate. The strength of the corroded parts in groups B, C and D is significantly lower than that of the uncorroded group and group A. However, the differences of mechanical properties of nine specimens in groups B, C and D are small. It can be found that the yield strength and ultimate strength of steel plate decrease with the increase of corrosion rate when the corrosion degree is low and the decline degree becomes less and less obvious.

Fig.18 shows the morphology of 12 specimens in groups A, B, C and D after tensile failure. There are obvious necking phenomena in all specimens after tensile failure. During the corrosion process, there were two sets of contact points between the specimen and the bracket, where obvious rust pits were formed. During the stretching process, stress concentration appeared at the edge of the corrosion pit, which made the stress distribution of the specimen uneven, thus the specimen broke at this position.

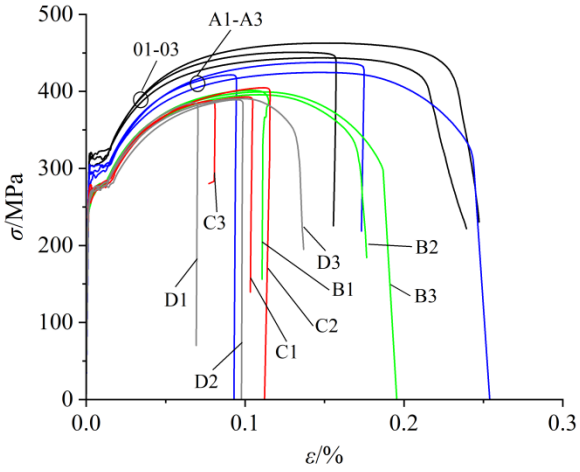


(a) Stress-strain curve

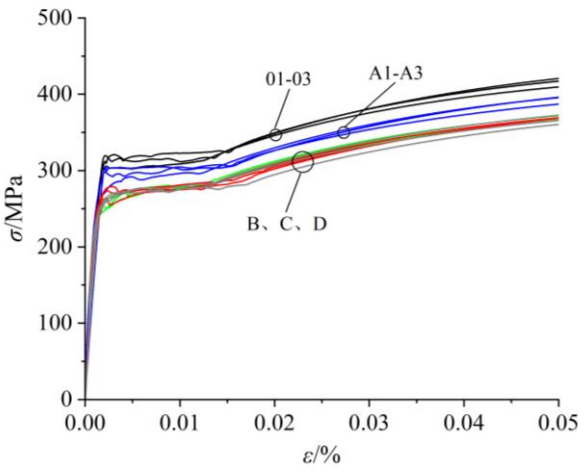


(b) Local enlarged view of stress-strain curve

**Fig. 17** Stress-strain curve of each specimen

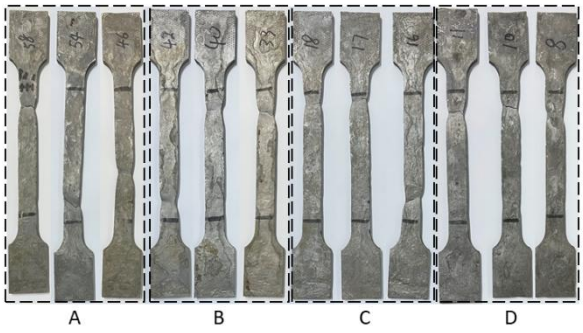


**Fig. 18** Tensile failure mode of corroded specimens

## 4. Evaluation methods of mechanical properties of corroded steel

The section mainly analyzes the evaluation methods of mechanical properties of corroded steel. Firstly, the mechanical properties of steel specimens during tensile test are extracted. Then, the mechanical properties of the corroded steel are evaluated according to corrosion rate, surface roughness and maximum pit size. Finally, the evaluation effects of different evaluation indexes are compared.

### *4.1. Mechanical property index*

The main mechanical properties of steel specimens are the nominal elastic modulus $E_s$, the nominal yield strength $f_y$, the nominal tensile strength $f_u$, the ratio of yield strength to tensile strength $f_y/f_u$, the elongation $A$ and the yield platform length $\varepsilon_A$. In order to facilitate the study of the changes of mechanical property indexes of steel after corrosion, the curves in Fig.17 are sorted out and the indexes obtained are listed in Table 7.

**Table 7**
Main mechanical property indexes of specimens in the tensile test

| No. | $\eta$/% | | $E_s$/GPa | $f_y$/MPa | $f_u$/MPa | $f_y/f_u$ | $A$/% | $\varepsilon_A$/% |
|---|---|---|---|---|---|---|---|---|
| 01 | 0 | | 197.70 | 319.60 | 450.88 | 0.709 | 22.41 | 1.310 |
| 02 | 0 | 0 | 223.80 | 305.80 | 443.65 | 0.689 | 22.07 | 1.046 |
| 03 | 0 | | 222.30 | 320.80 | 462.76 | 0.693 | 23.34 | 1.074 |
| A1 | 4.30 | | 203.20 | 291.70 | 421.50 | 0.692 | 19.76 | 0.873 |
| A2 | 4.46 | 4.31 | 206.70 | 305.30 | 437.72 | 0.697 | 23.03 | 1.221 |
| A3 | 4.18 | | 214.10 | 298.00 | 424.68 | 0.702 | 23.53 | 1.314 |
| B1 | 5.44 | | 204.80 | 279.60 | 401.43 | 0.697 | 19.76 | 1.124 |
| B2 | 5.40 | 5.59 | 224.80 | 280.98 | 395.76 | 0.640 | 16.97 | 1.143 |
| B3 | 5.91 | | 199.20 | 278.20 | 399.45 | 0.696 | 19.13 | 1.058 |
| C1 | 8.56 | | 239.40 | 278.90 | 392.93 | 0.710 | 18.60 | 1.145 |
| C2 | 8.26 | 8.56 | 213.80 | 273.80 | 404.82 | 0.676 | 17.24 | 1.026 |
| C3 | 8.86 | | 212.00 | 263.60 | 387.78 | 0.680 | 17.73 | 1.058 |
| D1 | 11.04 | | 233.20 | 277.24 | 385.20 | 0.625 | 17.20 | 1.077 |
| D2 | 11.36 | 11.02 | 222.00 | 277.92 | 389.31 | 0.697 | 20.23 | 1.056 |
| D3 | 10.67 | | 210.10 | 260.60 | 390.72 | 0.667 | 14.71 | 1.013 |

It can be seen from Table 7 that there are certain differences in the mechanical property indexes of specimens with the same corrosion duration. This is mainly due to the fact that rust is a complex electrochemical process. In the process of accelerated corrosion test, although the same environmental conditions are set, there are still significant differences in the formation position and size of corrosion pits on the surface of different specimens under the same corrosion time (as shown in Table 5). This difference at the microscopic level will lead to different degrees of stress concentration in the tensile process of the specimen, which leads to the dispersion of the tensile strength data. But in general, under the same corrosion rate, the difference of the mechanical properties of the specimen is less than 10%, the variability of the data is not large.

### *4.2. Corrosion rate index*

The relationship and law between mechanical properties of materials and $\eta$ can reveal the process of mechanical properties deterioration of steel during corrosion. Therefore, the relationship between each indicator and $\eta$ is established which is shown in Fig.19, where $E_{s0}$、$f_{y0}$、$f_{u0}$ are the maximum values of the corresponding indexes in the groups 01 ~ 03 of uncorroded specimens.

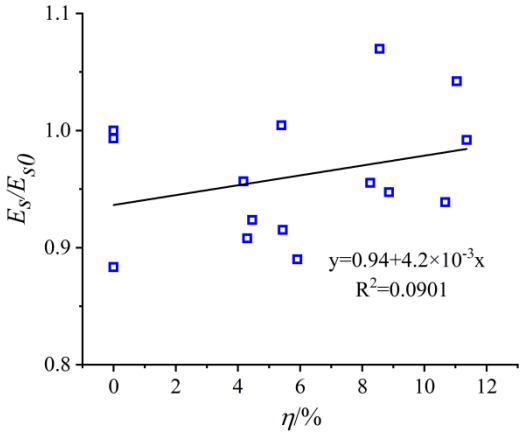


(a) Relationship between $E_s/E_{s0}$ and $\eta$

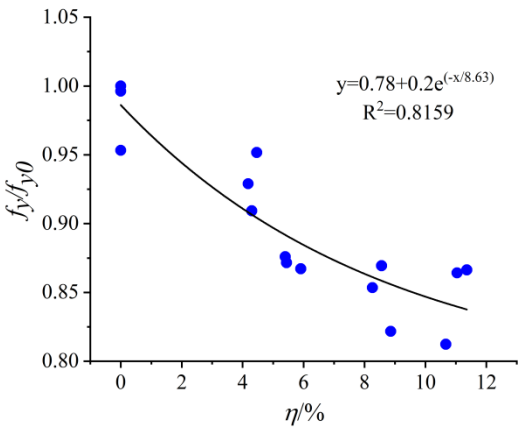


(b) Relationship between $f_y/f_{y0}$ and $\eta$

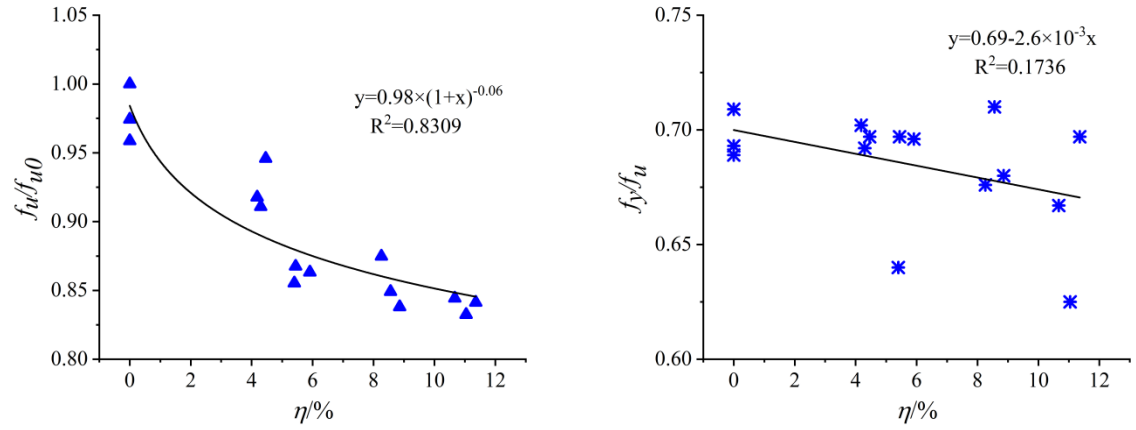


(c) Relationship between $f_u/f_{u0}$ and $\eta$ (d) Relationship between $f_y/f_u$ and $\eta$

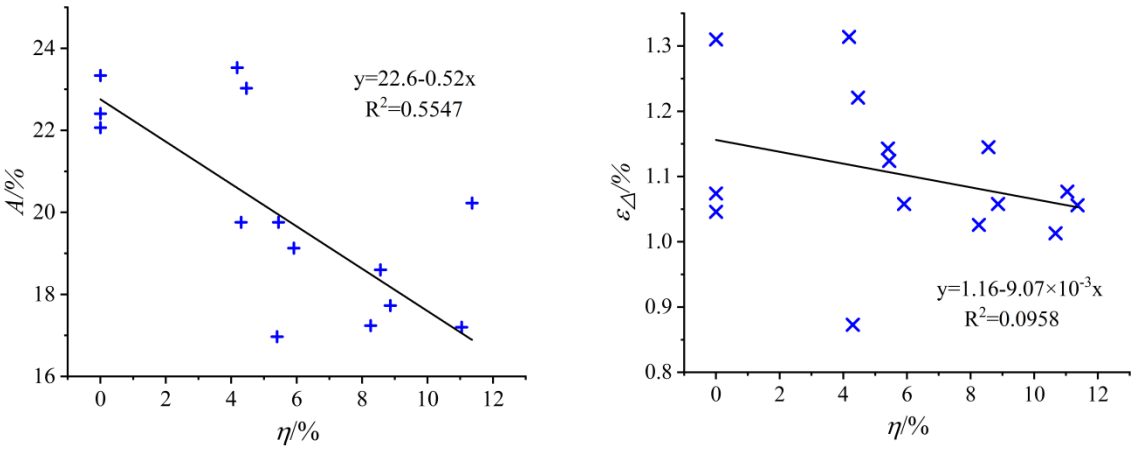


(e) Relationship between $A$ and $\eta$ (f) Relationship between $\varepsilon_\Delta$ and $\eta$

**Fig. 19** Relationship between mechanical properties of corroded components and $\eta$

According to Fig.19 (a), the relative elastic modulus $E_s/E_{s0}$ of the specimen fluctuates within the range of 0.85~1.1 with the increase of corrosion rate, corresponding to specific values of the elastic modulus from 197.7 to 239.4. The relative elastic modulus and corrosion rate of each group of specimens are fitted linearly, the correlation coefficient of the obtained relationship is only 0.0901, indicating a high degree of discreteness in the data. At the same time, the elastic modulus of the same group of specimens has great dispersion. Therefore, it can be considered that the corrosion process has little effect on the elastic modulus of the specimens.

For the data of corrosion rate and relative yield strength $f_y/f_{y0}$ and relative tensile strength $f_u/f_{u0}$ in Fig.19 (b) and Fig.19 (c), ExpDec1 and Pow2P2 functions are respectively used to fit the data and the following Eq. (6) and Eq. (7) are obtained.

$$\frac{f_y}{f_{y0}} = 0.78 + 0.2e^{(-\eta/8.63)}, R^2 = 0.8159 \quad (6)$$

$$\frac{f_u}{f_{u0}} = 0.98 + (1+\eta)^{-0.06}, R^2 = 0.8309 \quad (7)$$

It can be seen that correlation coefficients of the above relationships are both above 0.8, which indicates that the degree of fitting is relatively high, the yield strength and tensile strength of the steel specimen are significantly correlated with the rust rate. The $f_y$ and $f_u$ calculated by the above two equations have high reliability taking rust rate as the parameter.

The yield strength and tensile strength ratio $f_y/f_u$, elongation after fracture $A$ and yield platform length $\varepsilon_\Delta$ all decrease with the increase of corrosion rate as can be seen from (d), (e) and (f) in Fig 19. However, $R^2$ is low for the fitted curves due to the large dispersion of data. Therefore, general trend of $f_y/f_u$, $A$ and $\varepsilon_\Delta$ with the increase of $\eta$ can only be preliminarily explained, but cannot be evaluated and predicted by $\eta$.

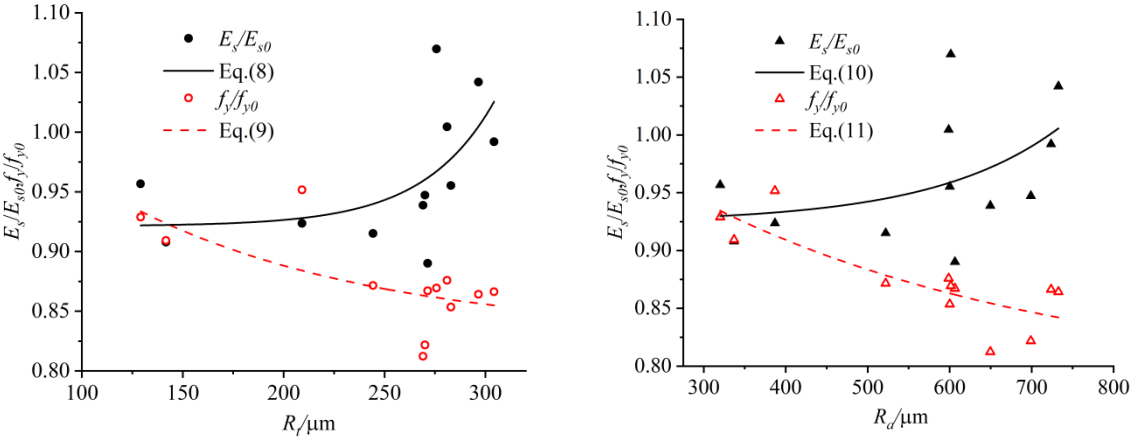


(a) Relationship of $E_s/E_{s0}$, $f_y/f_{y0}$ with $R_t$ (b) Relationship of $E_s/E_{s0}$, $f_y/f_{y0}$ with $R_a$

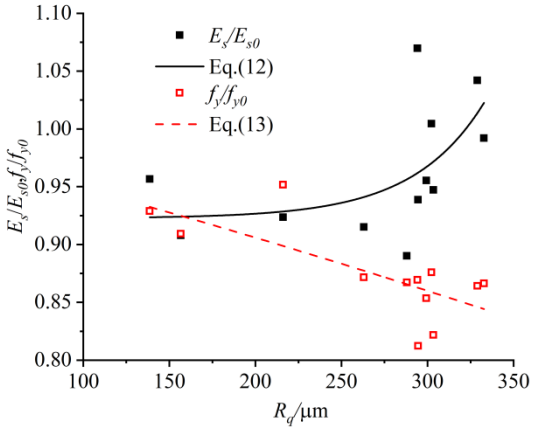


(c) Relationship of $E_s/E_{s0}$, $f_y/f_{y0}$ with $R_q$

**Fig. 20** Relationship of $E_s/E_{s0}$, $f_y/f_{y0}$ with roughness parameters

### *4.3. Surface morphology index*

Taking $\eta$ as an index to evaluate the corrosion degree of steel members is an ideal treatment for the surface morphology of the corroded parts, which simplifies the corrosion effect as the overall thinning effect of components. However, in the actual corrosion process, many rust pits are formed on the surface of corroded steel components, resulting in the obvious stress concentration phenomenon appears near the rust pits when the member is subjected to external load, which is the direct cause of the deterioration of mechanical properties of the members after corrosion. Therefore, the relationship between $E_s$, $f_y$ and surface roughness indexes of corroded components is established, as shown in Fig.20.

It can be seen that the values of $R_t$, $R_a$ and $R_q$ are small in the initial corrosion stage, while $E_s$ decreases slightly with the increase of roughness. $E_s$ increases accordingly when $R_t$, $R_a$ and $R_q$ exceed 250μm, 600μm and 250μm respectively. The stress state of the surface material of the member is changed from unidirectional stress state to triaxial stress state due to the formation of the rust pit, resulting in the increase of $E_s$. The yield strength of the specimen decreases nonlinearly with the increase of $R_t$, $R_a$ and $R_q$. The discreteness of $f_y$ increases with the increasing of $R_t$, $R_a$ and $R_q$ when $R_t$, $R_a$ and $R_q$ are greater than 250μm, 600μm and 250μm respectively, but it still shows a downward trend in general.

In order to verify the reliability of using specimen roughness parameters to evaluate $E_s$ and $f_y$, ExpDec1 function is used to fit the experimental data. The results are shown in the following equations.

① $R_t$ for the parameter

$$\frac{E_S}{E_{S0}} = 1.65\times10^{-5}\mathrm{e}^{R_t/34.78}, R^2 = 0.3345 \tag{8}$$

$$\frac{f_y}{f_{y0}} = 0.3\mathrm{e}^{(-R_t/122.83)} + 0.83, R^2 = 0.4483 \tag{9}$$

② $R_a$ for the parameter

$$\frac{E_S}{E_{S0}} = 7.04\times10^{-4}\mathrm{e}^{R_a/154.23} + 0.92, R^2 = 0.2252 \tag{10}$$

$$\frac{f_y}{f_{y0}} = 0.31\mathrm{e}^{(-R_a/436.83)} + 0.78, R^2 = 0.6744 \tag{11}$$

③ $R_q$ for the parameter

$$\frac{E_S}{E_{S0}} = 3.09\times10^{-5}\mathrm{e}^{R_q/41.18} + 0.92, R^2 = 0.3317 \tag{12}$$

$$\frac{f_y}{f_{y0}} = -0.54\mathrm{e}^{R_q/1400} + 1.52, R^2 = 0.5332 \tag{13}$$

Eq. (8), Eq. (10) and Eq. (12) are the fitting equations for evaluating $E_s$ with $R_t$, $R_a$ and $R_q$ as indexes, the correlation coefficients are 0.3345, 0.2252 and 0.3317 respectively. However, the discreteness of $E_s$ increases with the increase of $R_t$, $R_a$ and $R_q$. In general, the reliability of evaluating the $E_s$ of corroded steel by roughness parameters is not high, but it is better than the corrosion rate index.

Similarly, Eq. (9), Eq. (11) and Eq. (13) are the fitting equations for evaluating $f_y$ with $R_t$, $R_a$ and $R_q$ as indexes, the correlation $R^2$ are 0.4483, 0.6744 and 0.5332 respectively. The discreteness of $f_y$ is large when $R_t$, $R_a$ and $R_q$ are 250-300 μm, 600-750 μm and 250-350 μm respectively according to Fig.20. Therefore, the reliability of evaluating the yield strength of corroded components based on surface roughness is low.

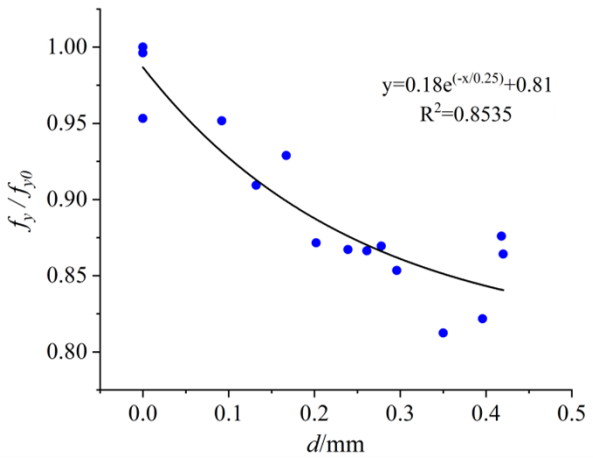


(a) Relationship between $f_y/f_{y0}$ and $d$

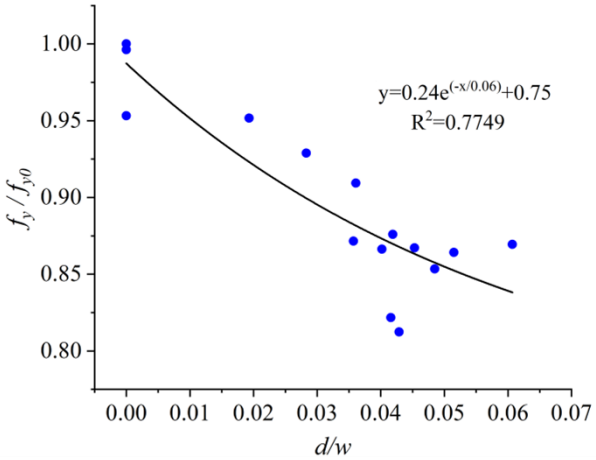


(b) Relationship between $f_y/f_{y0}$ and $d/w$

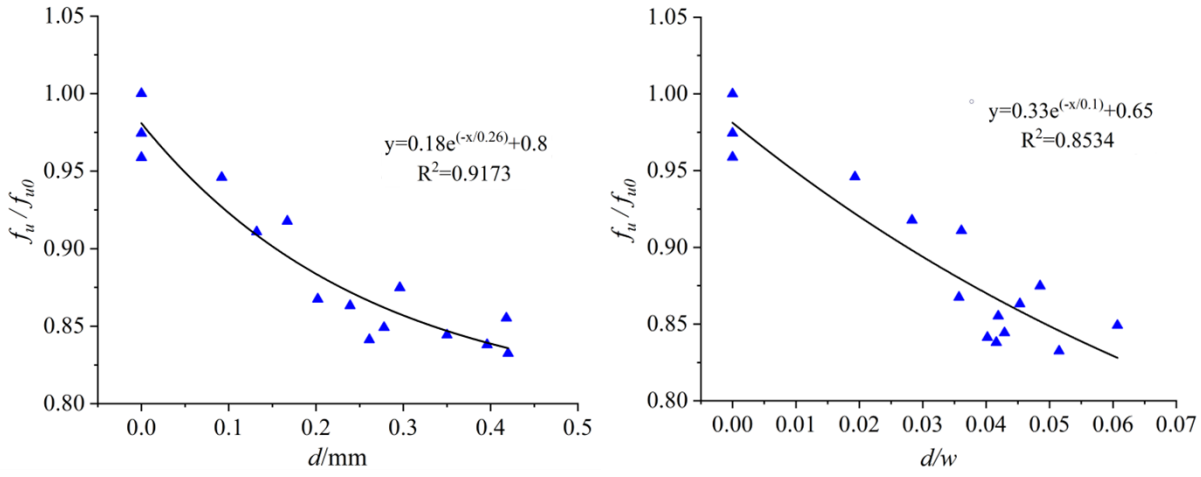


(c) Relationship between and $f_w/f_{u0}$ and $d$ (d) Relationship between $f_w/f_{u0}$ and $d/w$

**Fig. 21** Relationships between $f_y$ and $f_u$ and the size of the maximum rust pit

*4.4. Maximum rust pit size index*

There is a significant relationship between the microscopic level of corrosion surface and the mechanical properties of the component. It is found that $E_s$ has little correlation with the size of the largest rust pit. Therefore, the reliability evaluation of $f_y$ and $f_u$ based on the maximum pit size is mainly discussed. The relationship between $f_y$ and $f_u$ of corroded specimens and the size of the maximum rust pit is established, as shown in Fig 21.

It can be seen from Fig.21 that there is a significant nonlinear correlation between the mechanical properties of corrosion specimens and the size of the maximum rust pit. Equations (14), (15), (16) and (17) are obtained by numerical fitting of ExpDec1 function.

$$\frac{f_y}{f_{y0}} = 0.18^{-\frac{d}{0.25}} + 0.81, R^2 = 0.8535 \tag{14}$$

$$\frac{f_y}{f_{y0}} = 0.24^{-\frac{d}{0.06w}} + 0.75, R^2 = 0.7749 \tag{15}$$

$$\frac{f_u}{f_{u0}} = 0.18^{-\frac{d}{0.26}} + 0.8, R^2 = 0.9173 \tag{16}$$

$$\frac{f_u}{f_{u0}} = 0.33^{-\frac{d}{0.1w}} + 0.65, R^2 = 0.8534 \tag{17}$$

The fitting curves of $f_y$ and $f_u$ obtained by different parameters as evaluation indexes are compared as follows. For $f_y$, the correlation coefficient of Eq. (14) is 0.8535, which has higher accuracy than that of equations (6) and (15), while the fitting accuracy of equations (9), (11) and (13) is poor. It can be seen that in the fitting curve of $f_y$, the fitting curve obtained with the maximum rust pit depth as the index has better accuracy compared with the rust rate and the depth to width ratio of the maximum rust pit, while the fitting accuracy with the surface roughness as the index is poor. For $f_u$, the correlation coefficient of Eq. (16) is 0.9173, which is higher than Eq. (7) and Eq. (17), indicating that the maximum rust pit depth is the most accurate fitting curve, which is higher than the rust rate index and the maximum rust pit depth to width ratio index. In general, the maximum depth of rust pit on the surface of corroded components can be used as a parameter to evaluate the strength of corroded components with high precision. At the same time, when only the corrosion rate of the component is taken as the evaluation parameter, the obtained results also have high reliability. However, component strength cannot be accurately and reliably evaluated using only surface roughness parameters.

## 5. Discussion

In this paper, the morphologic changes of Angle steel during corrosion are discussed, the evaluation methods of corrosion rate and mechanical properties are obtained, which has certain guiding significance for engineering practice. In the future, corrosion Angle steel needs to be further explored and studied, including the following aspects:

1) The research carried out in this paper is based on the data obtained from the artificial accelerated corrosion test which is only applicable to Angle steel members whose surface corrosion is similar to that in this paper. The environment of Angle steel in engineering is different, so it is necessary to further improve the experiment under different climatic conditions.

2) The external load in the actual environment will further affect the degree of corrosion in the Angle steel rust zone. Therefore, the evaluation of corrosion degree and bearing capacity of multi-factor coupled lower Angle steel members can be explored.

## 6. Conclusions

In this paper, the standard tensile specimen of angle steel is taken as the research object and the corrosion specimen is prepared by accelerated corrosion test. The morphology data and mechanical properties of the corrosion specimen are obtained by contour scanning and tensile test at room temperature. The variation of roughness parameters and the deterioration of mechanical properties of steel specimens during corrosion are investigated, the variation laws of the surface of steel specimens at macro and micro levels during corrosion are explored. The relationship between corrosion rate, surface characteristics and mechanical indexes is established, the evaluation effect of different indexes on mechanical properties is compared. The main conclusions are as follows:

1) At the initial stage of corrosion, corrosion pits appear on the specimen surface and deepen continuously with the increase of corrosion rate, the surface roughness increases. When the corrosion rate of the specimen reaches a certain extent, the corrosion products hinder the further oxidation reaction of the specimen, the deepening speed of the rust pit slows down, the bottom becomes wider and the deeper pitting pits gradually develop into wider and deeper ulcer pits, The growth rate of the specimen surface roughness slows down.

2) Transmission tower components in operation are difficult to disassemble and weigh. Considering that the thickness of the rust layer has a significant relationship with the corrosion rate during the corrosion process, the corrosion rate of the component can be evaluated by measuring the maximum residual thickness of the component, so as to judge the degree of corrosion of the component.

3) The tensile test results show that for the mechanical properties of steel specimens, except that the elastic modulus is basically not affected by corrosion, the yield strength, tensile strength, elongation and other indicators show different degrees of deterioration with the increase of corrosion degree, which indicates that rust has a significant impact on the bearing capacity and deformation capacity of steel specimens.

4) The mechanical properties of corroded components are evaluated by corrosion rate, roughness parameters and maximum pit size. By comparing different evaluation equations, it can be found that the maximum depth of rust pit on the surface of corroded members is the most accurate evaluation index for yield strength and tensile strength, the obtained results also have high

reliability taking the corrosion rate of the component as the evaluation index. It is not reliable to evaluate the elastic modulus with each index.

**Acknowledgements**

The authors acknowledge the financial support provided by the "333 Talent Project of Hebei Province ”(C20231056)

**References**

[1] Gathimba N, Kitane Y. Characterization of surface topography of corroded steel members exposed to marine environments[C]//Corrosion and Prevention 2018.2018.
[2] Oszvald K, Tomka P, Dunai L. The remaining load-bearing capacity of corroded steel angle compression members[J].Journal of Constructional Steel Research, 2016, 120(apr.):188-198.
[3] Oszvald K, Dunai, László. Effect of corrosion on the buckling of steel angle members – experimental study[J]. Periodica Polytechnica Civil Engineering, 2012, 56(2).
[4] Beaulieu L, Legeron F, Langlois S. Compression strength of corroded steel angle members[J].Journal of Constructional Steel Research,2010,66(11):1366-1373.
[5] Surahyo A. Achieving Quality in Concrete Construction: Practical Problems and Solutions[M]. 2019.
[6] Garbatov Y, Soares C G, Parunov J, et al. Tensile strength assessment of corroded small scale specimens[J]. Corrosion science, 2014, 85:296-303.
[7] Jinchao J, Yong L, Zhao L, et al. Correlation between Laboratory-Accelerated Corrosion and Field Exposure Test for High-Strength Stainless Steels[J]. Materials, 2022,15(24):9075-9075.
[8] Bazan A, Galvez J, Reyes E, et al. Study of the rust penetration and circumferential stresses in reinforced concrete at early stages of an accelerated corrosion test by means of combined SEM, EDS and strain gauges [J]. Construction and Building Materials, 2018, 184: 655-67.
[9] Qi S, Yang D, Liang Z. Electrolytic accelerated corrosion morphology for structural steel based on an improved solution[J]. Corrosion Reviews,2021,39(4):373-386.
[10] Cheng D, Jin L, Xiqing Z, et al. Corrosion Dynamics of Low Carbon Steel in Salt Spray Environment[J]. Protection of Metals and Physical Chemistry of Surfaces,2023,59(4):729-735.
[11] Deliang K, Biao N, Shanhua X. Random Field Model of Corroded Steel Plate Surface in Neutral Salt Spray Environment[J]. KSCE Journal of Civil Engineering,2021,25(7):1-11.
[12] Qin G, Xu S, Yao D, et al. Study on the degradation of mechanical properties of corroded steel plates based on surface topography[J]. Journal of Constructional Steel Research,2016,125205-217.
[13] Yafeng Z, Gemma F, Elaine A, et al. Influence of Corrosion-Induced Damage on Mechanical Integrity and Load-Bearing Capability of Cemented Carbides[J]. Metals,2022,12(12):2104-2104.
[14] Qiang L, Xianyu J, Dongming Y, et al. Study of wiring method on accelerated corrosion of steel bars in concrete[J]. Construction and Building Materials,2020,(prepublish):121286-.
[15] Ou Y C, Susanto Y, Roh H. Tensile behavior of naturally and artificially corroded steel bars[J]. Construction and Building Materials, 2016, 103(Jan.30):93-104.
[16] Zhenye C, Shidong N, Wenbing H, et al. A study on static properties of high-performance steel after corrosion damage[J]. Journal of Constructional Steel Research,2023,207.
[17] Feng L, Zheng J, Guo Z, et al. Experimental study on the mechanical properties and ultimate strength of accelerated corrosion on hull plates[J]. Marine Structures,2024,95103591-.
[18] Sheng J, Xia J. Effect of simulated pitting corrosion on the tensile properties of steel[J]. Construction and Building Materials,2017,13190-100.
[19] Wang Y, Xu S, Wang H, et al. Predicting the residual strength and deformability of corroded steel plate based on the corrosion morphology[J]. Construction and Building Materials,2017,152777-793.
[20] Zhang Z, Xu S, Nie B, et al. Experimental and numerical investigation of corroded steel columns subjected to in-plane compression and bending[J]. Thin-Walled Structures,2020,151106735-106735.
[21] Zhiwei Z, Huajie W, Hongliang Q, et al. Comparative analysis and applicability of corrosion test methods for construction steel components[J]. Case Studies in Construction Materials,2023,18.
[22] Kumar V, Tiwari K S, Sharma N. Mechanical and surface characterization of interstitial-free steel corroded under wet-dry salt spray and immersion conditions: A comparative study[J]. Materials and Corrosion,2023,74(9):1289-1300.
[23] Songquan T, Huihui X ,Ni A, et al. Experimental investigation on corrosion fatigue crack initiation and growth of heat-treated U75V rail steel[J].International Journal of Fatigue,2024,178.
[24] Hiroaki T, Natsuko Y, Sayaka M, et al. Improved corrosion fatigue performance of 316L stainless steel by surface porosification[J]. Materials Letters,2023,353.
[25] Kainuma S, Jeong Y S , Ahn J H . Investigation on the stress concentration effect at the corroded surface achieved by atmospheric exposure test[J]. Materials Science and Engineering: A, 2014.
[26] An S L, Park C Y, Kim K H. An analytical approach to predict fatigue strength of corroded steel plates using random field-based corrosion surface modeling[J].Structures,2024,63106391-.
[27] Naftary G, Yasuo K. Effect of surface roughness on tensile ductility of artificially corroded steel plates[J]. Journal of Constructional Steel Research,2021,176106392-.
[28] Wei W, Yuan W, Jingqi H, et al. Mathematical Model of Surface Topography of Corroded Steel Foundation in Submarine Soil Environment[J]. Coatings,2022,12(8):1078-1078.
[29] Haipeng S, Jing L, Hao Z, et al. Multi-source data driven fatigue failure analysis and life prediction of pre-corroded aluminum–lithium alloy 2050-T8[J]. Engineering Fracture Mechanics,2023,292.
[30] Ren S, Kong C, Gu Y, et al. Measurement pitting morphology characteristic of corroded steel surface and fractal reconstruction model[J]. Measurement,2022,190.